

High Speed Vision-based 3D Reconstruction of Continuum Robots

Mohsen Moradi Dalvand, *Member, IEEE*, Saeid Nahavandi, *Senior Member, IEEE*, and Robert D. Howe, *Fellow, IEEE*

Abstract—Continuum robots offer better maneuverability and inherent compliance and are well-suited for surgical applications as catheters where gentle interaction with the environment is desired. However, sensing their shape and tip position is a challenge as traditional sensors cannot be employed in the same way that they are in rigid robotic manipulators. In this paper, a vision-based shape sensing algorithm for real-time 3D reconstruction of catheters based on the views of two arbitrary positioned cameras is presented. Customized high-speed algorithms are developed for the segmentation and feature extraction from the images. The algorithm is experimentally validated for accuracy by measuring the tip position, bending and orientation angles and for precision by estimating known 3D circular and elliptical shapes of the catheter. Experimental results demonstrate good accuracy and performance of the proposed high speed algorithms.

I. INTRODUCTION

Compared to traditional rigid-link robots, continuum robots offer advantages including better maneuverability and inherent compliance as they have continuum structure [1]. This makes them well-suited for a variety of applications from industrial inspections to minimally invasive surgery (MIS) operations where instruments must wind gently in between the tissues [2]–[4]. On the other hand, the flexibility and compliance feature of continuum robots makes it difficult and challenging to sense and control the shape and tip position of these robot manipulators. [5]. A few indirect methods relating internal actuator parameters to the tip position (average error between 17.4% to 57.4%) [6], [7] as well as direct methods including strain measurement [8], [9] and fiber optic sensors [10] have been introduced in the literature.

Vision-based shape sensing approaches have gained attention for quantifying the articulation of continuum robots by using the body- and/or tip-mounted fiducial markers that is more suitable for non-medical applications [7], [11], [12]. Vision-based techniques were also employed for the shape sensing and position control of

continuum robots in the field of medical robotics and instrumentation including steerable needles and catheters [13]–[16]. Different techniques based on the voxel-carving algorithm built upon the shape-from-silhouette technique [2], [17]–[19], affine shape of finite point configurations [20], [21], self-organizing map (SOM), growing self-organizing maps (GSOM) structures, and stereo SOM [19], [22] were also introduced. Although these algorithms are relatively robust and straightforward, they are computationally expensive [19].

The approach of 3D reconstruction of a quadratic curve by using two or more corresponding conics produced by projecting the curve onto image planes under perspective transformation was also studied [23]–[25]. This appealing approach seems to be computationally fast and well-suited for the application of 3D reconstruction of catheters and continuum robots and it, to the best knowledge of authors, hasn't been investigated before in literature for direct application in shape-sensing of catheters. In this work, based on this approach, a fast 3D reconstruction algorithm is proposed, implemented, experimentally validated and compared with other previously proposed methods. In Section II-A, the customized high-speed image processing algorithms are explained in detail. Section II-B presents the closed-form formulation for the 3D reconstruction process. Section III provides details about the experimental setup, procedure and results. Conclusion remarks are given in Section IV.

II. METHODS AND ALGORITHMS

The 3D reconstruction algorithm proposed in this research is based on the reconstruction of a quadratic curve representing the 3D shape of the catheter centerline from two arbitrary perspective projections [23]–[25]. The proposed method consists of four main steps. The first step is pre-processing of the two images acquired from both cameras which includes cropping and rectification of the images. The second step is to extract centerline points as well as tip point of the catheter from the two images using image processing techniques. The third step is to find the actual positions of the centerline and tip points on the image planes of the two cameras with respect to their coordinate frames using perspective transformation, determine the parameters of the 3D cone whose vertex is at the focal point of one of the cameras and passes through the points on the image plane of this camera, and finally obtain the closed-form

Mohsen M. Dalvand is with the Institute for Intelligent Systems Research and Innovation (IISRI), Deakin University, VIC 3216, Australia, and also with the Harvard Paulson School of Engineering and Applied Sciences, Cambridge, MA 02138, USA. (e-mail: mdalvand@seas.harvard.edu).

S. Nahavandi is with the Institute for Intelligent Systems Research and Innovation (IISRI), Deakin University, VIC 3216, Australia.

R. D. Howe is with the Harvard Paulson School of Engineering and Applied Sciences, Cambridge, MA 02138, USA.

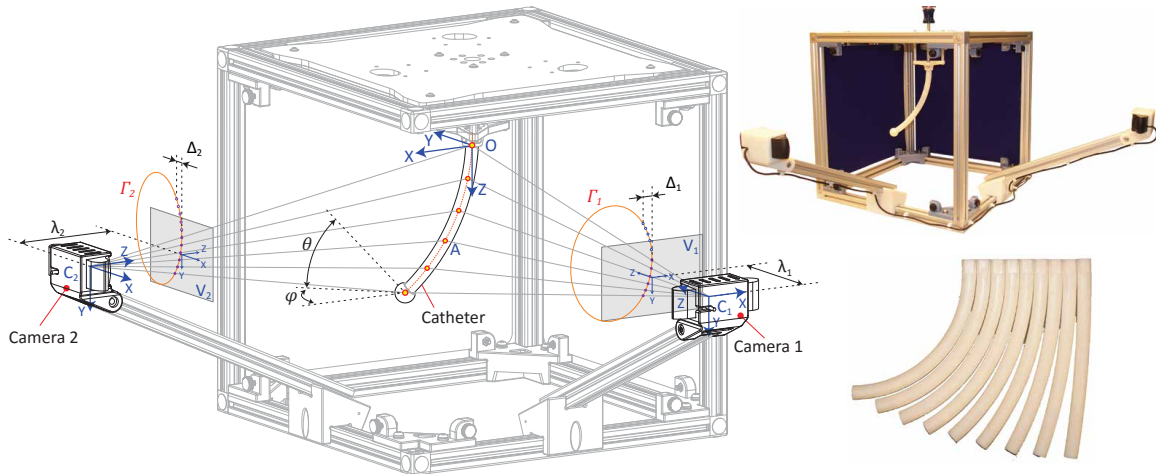


Fig. 1: Schematic description of the developed stereo imaging setup, the experimental setup, and the 3D printed catheter-shape tubes used in the experiments

analytical solutions of the intersection points of the ray lines of the other camera and this 3D cone surface. The fourth step is to utilise the obtained centerline points of the catheter to reproduce the 3D shape of the catheter and to extract its parameters including curvature, length, bending and orientation angles, and tip position. The schematic description of the proposed stereo imaging system is illustrated in Figure 1.

A. Image Processing Algorithms

The stereo vision system (Figure 1) consists of two cameras mounted on the structure so that they have clear views of the manipulation scene. The image backgrounds are covered by blue felt to simplify image preprocessing for experimental validation. The cameras are individually and also as a stereo system calibrated using the Camera Calibration Toolbox for Matlab [26]. The transformation matrix from the camera (C_ixyz) to the reference ($Oxyz$) coordinate frames were determined by using least-square technique and triangulating several known locations in R^3 with respect to the reference coordinate frame.

To facilitate high-speed measurement and control of the catheters, a special emphasis has been put on the optimization of the image processing algorithms allowing the implementation in real-time. The image processing algorithms in this research involve three main steps of (a) preprocessing; (b) tip point detection; and (c) centerline points extraction. The proposed algorithms are described in detail in the flowchart of the Figure 2 that includes examples of the memory blocks image1 to image13 used in this flowchart.

The preprocessing procedure comprises of removing lens distortions from the images, cropping (Figure 2-image1), thresholding and removing the blue backgrounds, removing the noise, and finding the position of the origin points by finding the location of the

middle point of the the most top-right and most top-left white points in the images. A customized algorithm was designed to find the position of the tip point as the conventional methods like Hough transform for finding circles was found to be sensitive to noise resulting in the detection of features with different properties for the images from identical views. As described in the flowchart (Figure 2), the region of interest (ROI) of the tip (Figure 2-image3) is found by detecting the most bottom white point in the binary image of the isolated catheter. The tip position is then estimated by applying a distance transform to the ROI (Figure 2-image4). A mask image containing the line joining the origin point to the estimated tip point and its perpendicular line at the tip point is produced (Figure 2-image6). By applying bitwise AND operation of the Canny edge of the ROI (Figure 2-image5) and the mask image, three points on the edge of the tip circle are obtained (Figure 2-image7). These points are then used to find the best fitted circle (Figure 2-image8) which gives the accurate position of the tip point. Once the tip point is detected, the tip circle is removed from the image in order to isolate the catheter tube for the center line detection algorithm.

To reproduce the centerline of the catheter from the images, several techniques can be employed including SOM, detecting ridges using a distance transform, calculating the Voronoi diagram, thinning layer by layer erosion, and etc [17], [19], [27]. While in practice these techniques work well, to lower the execution time, a customized algorithm was developed (Figure 2). This algorithm begins with applying a mask containing a circular arc centered at the origin point to the binary images of the isolated catheter. This operation produces an image containing a small contour of the catheter in the form of a circular arc (Figure 2-image12-1). The center of mass of this contour belongs to the center path of the catheter. By repeating this procedure (Fig-

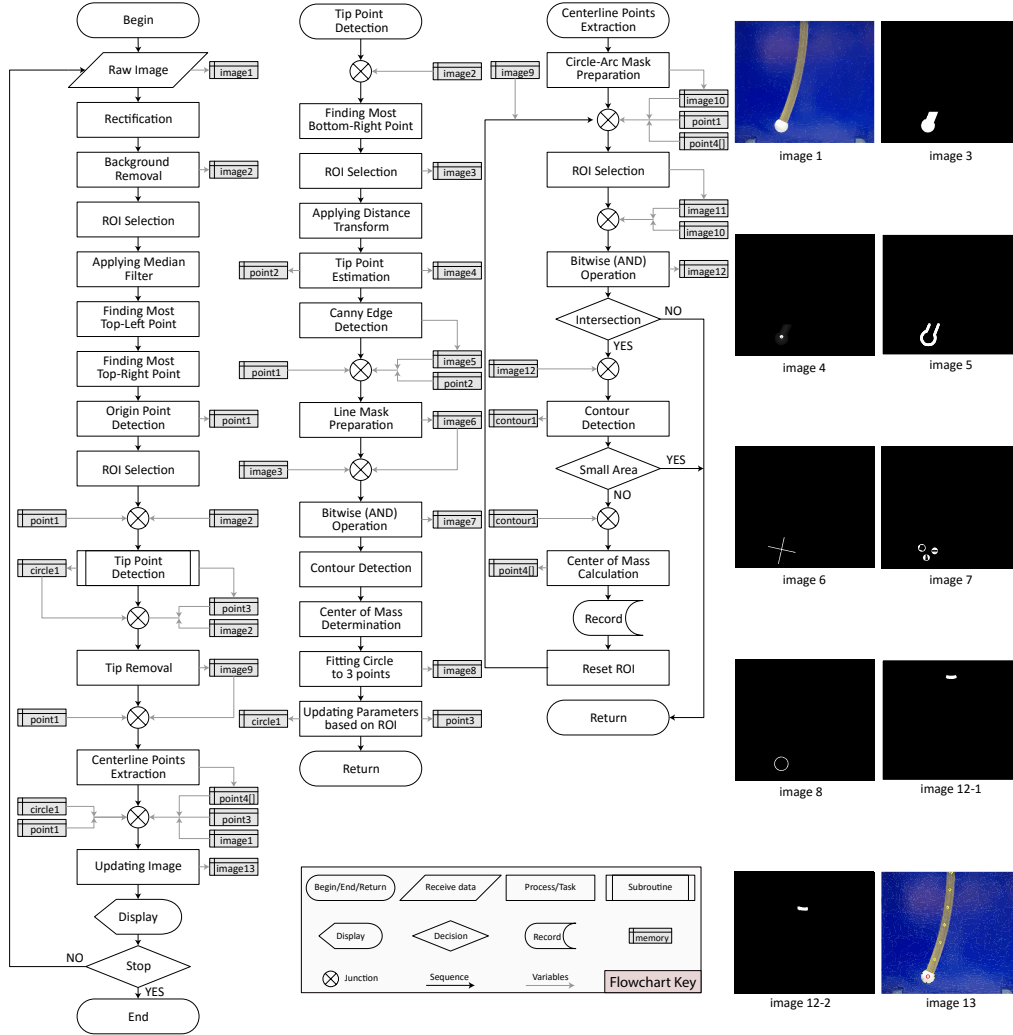


Fig. 2: Flowchart of the proposed image processing algorithms and examples of the memory blocks

ure 2-image12-2) until the area of the contour is zero, several points on the centerline are obtained (Figure 2-image13). The number of the points can be adjusted by changing the radius of the circular arc used as the mask. The extracted centerline points of the catheter that includes the origin and tip points will be used in reconstruction algorithm.

B. Reconstruction Algorithm

In Figure 1, $C_i xyz$ ($i = 1, 2$) is the rectangular Cartesian coordinate of the i -th camera, V_i is the virtual image plane of the i -th camera, $Oxyz$ is the reference frame, and A is an arbitrary point in R^3 from the catheter centerline. The proposed reconstruction algorithm is presented in the flowchart of the Figure 3.

The actual 3D position of the centerline points of the catheter projected upon the virtual image planes V_i (A_{v_i}) are obtained using the perspective equation. The best fitted quadratic curve Γ_i to the n projected points

A_{v_i} on the virtual image plane of the i -th camera that is in the form of an ellipse is then determined by applying least square technique [28]. Any point A_{v_i} on the curve Γ_i also belongs to the line $C_i A$ as it is demonstrated in Figure 1. By using lines $C_i A$ and the ellipse Γ_i , the elliptical cone Φ_i is derived. The vertex of this cone is the focal point of the i -th camera and its intersection with the virtual plane V_i is the ellipse Γ_i . Among the two intersection points of the line $C_i A$ and the elliptical cone Φ_i , the closer point to the reference frame origin (point O) along the z axis of the j -th camera coordinate belongs to the catheter centerline (Figure 1). Coordinates of the intersection point with respect to the reference frame at point O is then determined by applying the transformation matrix of the coordinate systems of the j -th camera to the reference frame. Using same algorithm, other points of the centerline are obtained and can be used to find the best fitted curve representing the curvature of the

catheter in 3D space. This curve will then be used to obtain other features of the catheter including length.

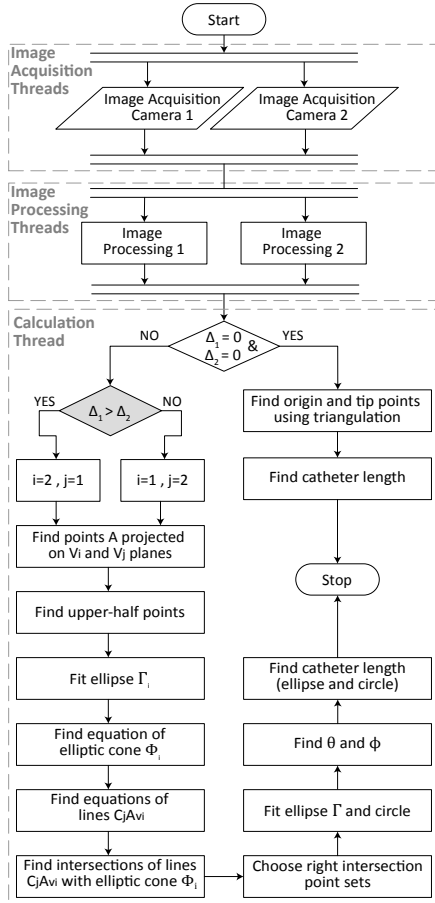


Fig. 3: 3D reconstruction algorithm based on the closed-form analytical solution of the reconstruction of quadratic curves in 3D space from two arbitrary perspective projections

Figure 4 presents the 3D plots illustrating the reconstruction algorithm for a catheter with the bending angle of 50 deg in the orientation angles of 30 deg (Figure 4-left) and 60 deg (Figure 4-right). The 3D elliptical cones and the ray-lines of the cameras selected for the reconstruction algorithm are demonstrated in these figures. As described in the reconstruction flowchart (Figure 2), amongst the two 3D elliptical cones, one is chosen based on the parameter Δ_i (Figure 1). For the catheter-shape tube positioned in the orientation angle of 30 deg (Figure 4-left), the catheter is more exposed to the first (right) camera. This makes the cone of this camera more suitable for the reconstruction algorithm. When the orientation angle is larger than 45 deg for the first quadrant, the second (left) camera has better view of the catheter-shape tube with more horizontally stretched cone (Figure 4-right). Therefore, in this case the left camera cone is employed for the reconstruction algorithm (Figure 4-right).

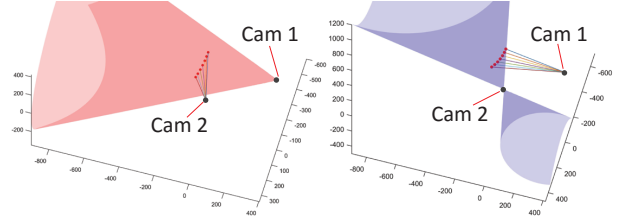


Fig. 4: 3D plots of the reconstruction cones and ray-lines for catheters with orientation angles of 30 deg (left) and 60 deg (right)

III. EXPERIMENTS

A stereo vision system consisting of two webcams (Logitech Webcam C930e; $1920 \times 1080 \text{ pixels} @ 30 \text{ fps}$) is integrated into the experimental setup (Figure 1). In the first experiment, 3D printed catheter-shape tubes (Figure 1) with known bending angles of $10, 30, 50,$ and 70 deg (160 mm long and 12 mm in diameter) are manually positioned in the orientation angles of $30, 60, 120, 150, 210, 240, 300,$ and 330 deg and the image processing and reconstruction algorithms are performed. In the second experiment, the tubes with the bending angles of $10, 20, 30, 40, 50, 60,$ and 70 deg were tested by manually rotating them in front of the cameras while the proposed shape sensing algorithms were determining curvature and geometry of the tubes in real-time. The measurement was repeated and recorded three times.

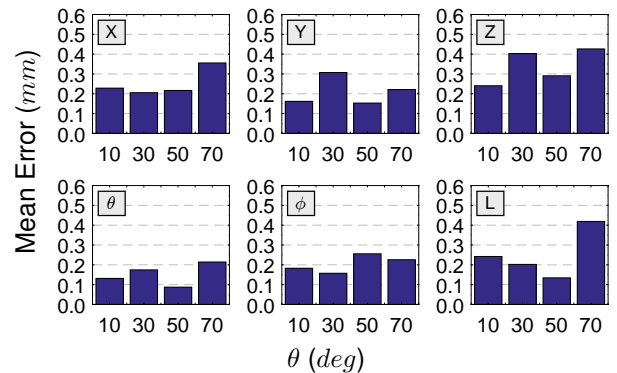


Fig. 5: Mean errors of $x, y,$ and z coordinates of the tip point and bending angles (θ), orientation angles (ϕ), and length (L) measured for the tubes with the bending angles of $10, 30, 50,$ and 70 deg

Figures 5 presents the mean of the measurement errors for $x, y,$ and z coordinates of the tip point, bending and orientation angles, and length of the catheter across the workspace for different bending angles of $10, 30, 50,$ and 70 deg . Figure 6 presents examples of the measurement errors in height of the tip point, bending angles, and length of the tube with 30 deg bending

angle, respectively from top to bottom. As it is clear from these figures, the mean of the measurement errors for all the parameters x , y , z , θ , ϕ , L are less than 0.5 mm and 0.5 deg .

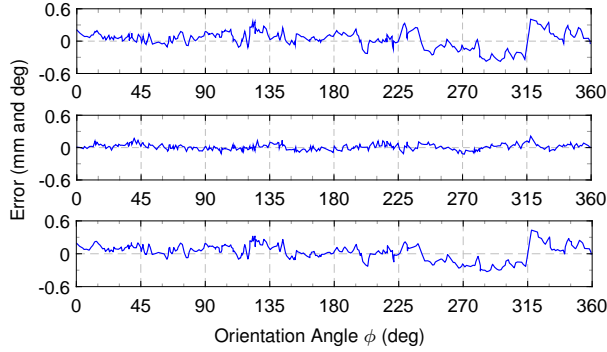


Fig. 6: Sample measurement errors of z coordinate of the tip point, bending angle, and length of the tube with 30 deg bending angle in the second experiment, respectively from top to bottom

The execution time required for the entire image processing algorithms proposed in this research is measured to be 2.75 millisecond for the two images with the resolution of $1920 \times 1080 \text{ pixels}$, and for the 3D reconstruction algorithm is measured to be 2.25 millisecond allowing the processing rate of around 200 fps . However, the web cameras used in the experimental setup developed in this research are limited to 30 fps .

To compare the results from the proposed algorithm with those of the previously proposed researches, a sampling of the diversity of the vision-based algorithms for 2D/3D reconstruction of catheters/continuum robots/flexible manipulators is compiled in Table I. Some of the results listed in this table are promising in terms of accuracy, however, low speed, dependency to tip- or body-mounted fiducial markers, physical grids, or high number of required cameras/images restrict their capabilities for high speed application like motion compensation cardiac catheters.

IV. CONCLUSION

In this paper, a vision-based shape sensing algorithm for real-time 3D reconstruction of cardiac catheters using two arbitrary perspective views based on the closed-form analytical solution for the reconstruction of quadratic curves in 3D space was presented. The execution time of the 3D reconstruction algorithm is measured to be 2.25 millisecond . The proposed algorithm combined with a high-speed image processing algorithm similar to the one proposed here allows the processing rate of around 200 fps or even more. The experimental results demonstrated the maximum measurement errors of 0.5 mm for the tip position and length and 0.5 deg for the bending and orientation angles of the catheter-shape rapid-prototyped tubes with known geometry and curvature. The high-speed, accuracy, and no dependency to body-mounted fiducial markers in the proposed system makes it a potential solution for the shape-sensing of motion compensation cardiac catheters.

TABLE I: Summary of previous studies

| Author(s) | Application | Algorithm / Technique | Camera Type | # of Camera | Resolution | Software | Accuracy | Speed |
|------------------------|-----------------|-------------------------|---------------|-------------|--------------------|----------|---|--|
| Rucker [29] | Medical | Body-Mounted Fiducial | Sony XCD-X710 | 2 | 1024×768 | Matlab | 2.2 mm | .. |
| Lee [30] | Medical | Epipolar Reconstruction | X-Ray | 2 | ... | Matlab | $2.5 - 3 \text{ pixel}$ | $596.7+134 \text{ ms}$ 1.36 fps |
| Hannan [31] | Not Medical | Body-Mounted Fiducial | Dalsa CCD | 1 | ... | ... | ... | 1.67 ms 598.8 fps |
| Camarillo [17], [18] | Medical | Shape-from-Silhouette | Webcam | 3 | 640×480 | OpenCV | $0.24 - 0.77 \text{ mm}$ | $250-333.3 \text{ ms}$ $3-4 \text{ fps}$ |
| Berthilsson [20], [32] | General | Affine Shape | ... | 6-13 | ... | ... | $1/20 \text{ pixel}$ | ... |
| Webster [12] | Medical | Tip-Mounted Fiducial | Sony XCD-X710 | 2 | ... | Matlab | ... | 66.6 ms 15 fps |
| Martinsson [33] | Quality Control | Fixed Complexity Model | ... | 20 | 1392×1040 | ... | 0.157 mm | ... |
| Hong [34] | General | Symmetric Curves | ... | 1 | ... | Matlab | ... | 10 min 0.001 fps |
| Croom [19] | Medical | Self-Organizing Maps | Sony XCD-X710 | 2 | 1024×768 | Matlab | $1.53-3.14 \text{ M}^1$ $0.31-0.93 \text{ Sd}^2$ | 248 ms 4 fps |
| This Research | Medical | Closed-Form Solution | Webcam | 2 | 1920×1080 | OpenCV | 0.6 Mx^3 $0.2 \text{ M}^1 \text{ \& Sd}^2$ | $2.75+2.25 \text{ ms}$ 202 fps |

¹Mean error in mm

²Standard deviation error in mm

³Maximum error in mm

REFERENCES

- [1] D. Trivedi, C. D. Rahn, W. M. Kier, and I. D. Walker, "Soft robotics: Biological inspiration, state of the art, and future research," *Applied Bionics and Biomechanics*, vol. 5, no. 3, pp. 99–117, 2008.
- [2] D. B. Camarillo, C. F. Milne, C. R. Carlson, M. R. Zinn, and J. K. Salisbury, "Mechanics modeling of tendon-driven continuum manipulators," *Robotics, IEEE Transactions on*, vol. 24, no. 6, pp. 1262–1273, 2008.
- [3] R. J. Webster, J. M. Romano, and N. J. Cowan, "Mechanics of precurved-tube continuum robots," *Robotics, IEEE Transactions on*, vol. 25, no. 1, pp. 67–78, 2009.
- [4] K. Ikuta, T. Hasegawa, and S. Daifu, "Hyper redundant miniature manipulator" Hyper Finger" for remote minimally invasive surgery in deep area," in *Robotics and Automation, 2003. Proceedings. ICRA'03. IEEE International Conference on*, vol. 1. IEEE, 2003, pp. 1098–1102.
- [5] G. Robinson and J. B. C. Davies, "Continuum robots-a state of the art," in *Robotics and Automation, 1999. Proceedings. 1999 IEEE International Conference on*, vol. 4. IEEE, 1999, pp. 2849–2854.
- [6] B. A. Jones and I. D. Walker, "Kinematics for multisection continuum robots," *Robotics, IEEE Transactions on*, vol. 22, no. 1, pp. 43–55, 2006.
- [7] V. K. Chitrakaran, A. Behal, D. M. Dawson, and I. D. Walker, "Setpoint regulation of continuum robots using a fixed camera," in *American Control Conference, 2004. Proceedings of the 2004*, vol. 2. IEEE, 2004, pp. 1504–1509.
- [8] J. Lee, S. N. Sponberg, O. Y. Loh, A. G. Lamperski, R. J. Full, and N. J. Cowan, "Templates and anchors for antenna-based wall following in cockroaches and robots," *Robotics, IEEE Transactions on*, vol. 24, no. 1, pp. 130–143, 2008.
- [9] S. Leleu, H. Abou-Kandil, and Y. Bonnassieux, "Piezoelectric actuators and sensors location for active control of flexible structures," *Instrumentation and Measurement, IEEE Transactions on*, vol. 50, no. 6, pp. 1577–1582, 2001.
- [10] K. T. V. Grattan and T. Sun, "Fiber optic sensor technology: an overview," *Sensors and Actuators A: Physical*, vol. 82, no. 1, pp. 40–61, 2000.
- [11] T. Matsuno, T. Fukuda, and F. Arai, "Flexible rope manipulation by dual manipulator system using vision sensor," in *Advanced Intelligent Mechatronics, 2001. Proceedings. 2001 IEEE/ASME International Conference on*, vol. 2. IEEE, 2001, pp. 677–682.
- [12] R. J. Webster III, J. P. Swensen, J. M. Romano, and N. J. Cowan, "Closed-form differential kinematics for concentric-tube continuum robots with application to visual servoing," in *Experimental Robotics*. Springer, 2009, pp. 485–494.
- [13] R. J. Webster, J. Memisevic, and A. M. Okamura, "Design considerations for robotic needle steering," in *Robotics and Automation, 2005. ICRA 2005. Proceedings of the 2005 IEEE International Conference on*. IEEE, 2005, pp. 3588–3594.
- [14] V. Kallem and N. J. Cowan, "Image-guided control of flexible bevel-tip needles," in *Robotics and Automation, 2007 IEEE International Conference on*. IEEE, 2007, pp. 3015–3020.
- [15] D. Glozman and M. Shoham, "Image-guided robotic flexible needle steering," *Robotics, IEEE Transactions on*, vol. 23, no. 3, pp. 459–467, 2007.
- [16] H.-J. Bender, R. Manner, C. Poliwoda, S. Roth, and M. Walz, "Reconstruction of 3D catheter paths from 2D X-ray projections," in *Medical Image Computing and Computer-Assisted Intervention—MICCAI'99*. Springer, 1999, pp. 981–989.
- [17] D. B. Camarillo, K. E. Loewke, C. R. Carlson, and J. K. Salisbury, "Vision based 3-D shape sensing of flexible manipulators," in *Robotics and Automation, 2008. ICRA 2008. IEEE International Conference on*. IEEE, 2008, pp. 2940–2947.
- [18] D. B. Camarillo, C. R. Carlson, and J. K. Salisbury, "Configuration tracking for continuum manipulators with coupled tendon drive," *Robotics, IEEE Transactions on*, vol. 25, no. 4, pp. 798–808, 2009.
- [19] J. M. Croom, D. C. Rucker, J. M. Romano, and R. J. Webster, "Visual sensing of continuum robot shape using self-organizing maps," in *Robotics and Automation (ICRA), 2010 IEEE International Conference on*. IEEE, 2010, pp. 4591–4596.
- [20] R. Berthilsson, K. Astrom, and A. Heyden, "Projective reconstruction of 3d-curves from its 2d-images using error models and bundle adjustments," in *Proceedings of the Scandinavian Conference on Image Analysis*, vol. 2. proceedings published by various publishers, 1997, pp. 581–588.
- [21] G. Sparr, "Simultaneous reconstruction of scene structure and camera locations from uncalibrated image sequences," in *Pattern Recognition, 1996., Proceedings of the 13th International Conference on*, vol. 1. IEEE, 1996, pp. 328–333.
- [22] R. L. M. E. do Rego, A. F. R. Araujo, and F. B. de Lima Neto, "Growing self-organizing maps for surface reconstruction from unstructured point clouds," in *Neural Networks, 2007. IJCNN 2007. International Joint Conference on*. IEEE, 2007, pp. 1900–1905.
- [23] K. Kanatani and W. Liu, "3D interpretation of conics and orthogonality," *CVGIP: Image Understanding*, vol. 58, no. 3, pp. 286–301, 1993.
- [24] M. Xie and M. Thonnat, "A theory of 3D reconstruction of heterogeneous edge primitives from two perspective views," in *Computer Vision—ECCV'92*. Springer, 1992, pp. 715–719.
- [25] R. Balasubramanian, S. Das, and K. Swaminathan, "Reconstruction of quadratic curves in 3-D from two or more perspective views," *Mathematical problems in Engineering*, vol. 8, no. 3, pp. 207–219, 2002.
- [26] J.-Y. Bouguet, "Camera Calibration Toolbox for Matlab." [Online]. Available: http://www.vision.caltech.edu/bouguetj/calib_{_}doc/index.html
- [27] G. S. Kumar, P. K. Kalra, and S. G. Dhande, "Curve and surface reconstruction from points: an approach based on self-organizing maps," *Applied Soft Computing*, vol. 5, no. 1, pp. 55–66, 2004.
- [28] R. Halir and J. Flusser, "Numerically stable direct least squares fitting of ellipses," in *Proc. 6th International Conference in Central Europe on Computer Graphics and Visualization. WSCG*, vol. 98. Citeseer, 1998, pp. 125–132.
- [29] D. C. Rucker, "THE MECHANICS OF CONTINUUM ROBOTS: MODEL-BASED SENSING AND CONTROL," Ph.D. dissertation, Vanderbilt University, 2011.
- [30] W.-S. Lee and T. Poston, "Rapid 3D tube reconstruction from nearby views," in *Fifth International Conference in Central Europe in Computer Graphics and Visualization*. Citeseer, 1997, pp. 262–271.
- [31] M. W. Hannan and I. D. Walker, "Real-time shape estimation for continuum robots using vision," *Robotica*, vol. 23, no. 05, pp. 645–651, 2005.
- [32] R. Berthilsson and K. Astrom, "Reconstruction of 3d-curves from 2d-images using affine shape methods for curves," in *Computer Vision and Pattern Recognition, 1997. Proceedings., 1997 IEEE Computer Society Conference on*. IEEE, 1997, pp. 476–481.
- [33] H. Martinsson, F. Gaspard, A. Bartoli, and J.-M. Lavest, "Reconstruction of 3d curves for quality control," in *Image Analysis*. Springer, 2007, pp. 760–769.
- [34] W. Hong, Y. Ma, and Y. Yu, "Reconstruction of 3-D symmetric curves from perspective images without discrete features," in *Computer Vision-ECCV 2004*. Springer, 2004, pp. 533–545.